Computer-Aided Design and Improved Performance of Tunable Ferrite-Loaded E-Plane Integrated Circuit Filters for Millimeter-Wave Applications

JAROSLAW UHER, FRITZ ARNDT, SENIOR MEMBER, IEEE, AND JENS BORNEMANN, MEMBER, IEEE

***Abstract*—The modal scattering matrix method is applied for the rigorous computer-aided design of low-insertion-loss magnetically tunable E-plane metal insert filters with improved characteristic, where only the resonator sections are loaded with ferrite slabs, and large-gap finline filters on a ferrite substrate of moderate width, for millimeter wave applications. The design method is based on field expansion in suitably normalized eigenmodes which yields directly the modal scattering matrix of key building block discontinuities, which are then appropriately combined for modeling the complete filter structure. The theory includes both the higher order mode interaction of all discontinuities involved and the finite thickness of the metal inserts, or metallization, respectively. Optimized data are given for magnetically tunable *Ku*-band (12–18 GHz), *Ka*-band (26–40 GHz), and *V*-band (50–75 GHz) metal insert and finline filter examples. The theory is verified by measurements of *Ku*-band metal insert and finline filters, utilizing ferrite TTI-2800 and TTVG 1200 materials.**

I. Introduction

TUNABLE waveguide filters, where the bandpass characteristic may be controlled within a desired frequency range, are of considerable practical interest for many applications [1]–[12]. Common techniques include sliding walls [1], varactor diodes [2], YIG resonators [1], [3]–[5], ferrite-slab-loaded evanescent-mode waveguide sections [6], [7], and hexagonal ferrite materials [8]–[10]. Although providing wide tuning ranges, the application of YIG tuned filters may often be restricted by the relatively narrow band selectivity available, the low power handling capability, and the magnetic saturation of the accessible materials, which causes limitations, especially at higher frequencies [1], [3]–[5], [7], [8]. Hexagonal ferrites utilize the large anisotropy to reduce the magnetic field required and, hence, are also appropriate for higher frequencies. However, the known tunable filter designs using hexagonal ferrite [8]–[10], [39], show relatively high insertion loss. Tunable evanescent filter techniques have hitherto been restricted to X-band (8–12 GHz) designs [6], [7]. Moreover, the capacitive posts and screws used in the below-cutoff sections [6], [7], may require relatively expensive fabrication methods and postassembly adjustments.

More recently, magnetically tunable E-plane integrated circuit filters have been introduced [11], [12], which are particularly appropriate for low-cost photolithographic fabrication techniques and for millimeter-wave applications. These are the E-plane metal insert filter with lateral ferrite inserts and the large-gap finline filter on a ferrite substrate. This paper describes new designs of millimeter-wave, magnetically tunable E-plane integrated circuit filters offering improved performance. The E-plane metal insert filter where only the resonator sections are loaded with ferrite slabs (Fig. 1(a)) achieves improved stopband characteristics. The large-gap finline filter on a TT86-6000 ferrite substrate of small width ($w = 0.22$ mm) yields low-insertion-loss millimeter-wave characteristics.

The design combines the advantages of printed circuit technology [13]–[21] with the high power capability of tunable ferrite-slab-loaded waveguide filters [6], [7]. Moreover, the exact design theory permits high-precision manufacturing by etching techniques without the necessity of postassembly "trial-and-error" adjustment methods. Furthermore, these types of filters, which are also suitable for a large number of resonators, may complement advantageously the more narrow band YIG filters, when relatively large bandwidth designs combined with moderate tuning ranges are required.

Many refined design methods for printed E-plane circuit filters without ferrite-loaded waveguide sections [13]–[21] and for ferrite-slab-loaded waveguides [22]–[30] are available. The computer-aided design of the magnetically tunable E-plane integrated circuit filters presented in this paper (Fig. 1) is based on the modal S matrix method [11], [12], [15], [16], [21], [28]–[30], which has already proved to be highly appropriate for the accurate design of millimeter-wave components since higher order mode cou-

Manuscript received April 8, 1988; revised August 17, 1988. This work was supported by the German Research Society (DFG) under Contract Ar138/6-1.

J. Uher was with the Microwave Department, University of Bremen, Bremen, West Germany. He is now with the Department of Electrical and Computer Engineering, University of Ottawa, Ottawa, Ont., Canada K1N 6N5.

F. Arndt is with the Microwave Department, University of Bremen, D-2800 Bremen 33, West Germany.

J. Bornemann was with the Microwave Department, University of Bremen, Bremen, West Germany. He is now with the Department of Electrical and Computer Engineering, University of Victoria, Victoria, B.C., Canada V8W 2Y2.

IEEE Log Number 8824204.

0018-9480/88/1200-1841$01.00

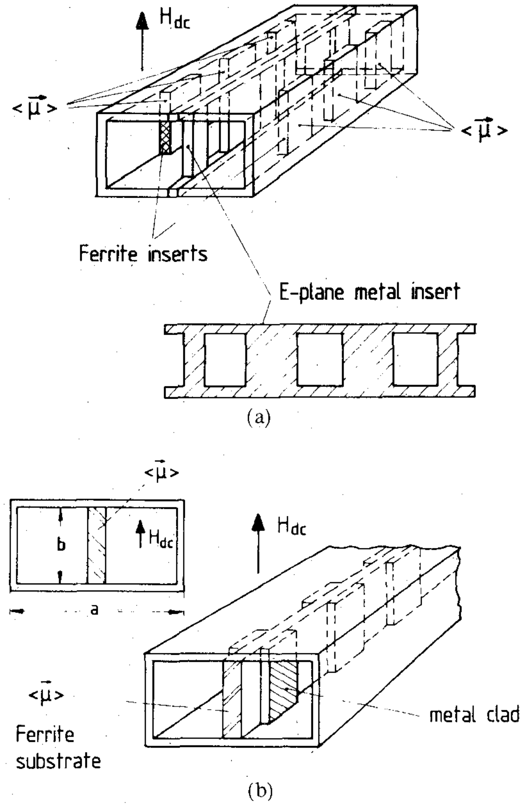

Fig. 1. Magnetically tunable E-plane integrated circuit filters with improved performance. (a) E-plane metal insert filter with ferrite-loaded resonator sections. (b) Low-insertion-loss large-gap finline filter on a ferrite substrate of small width.

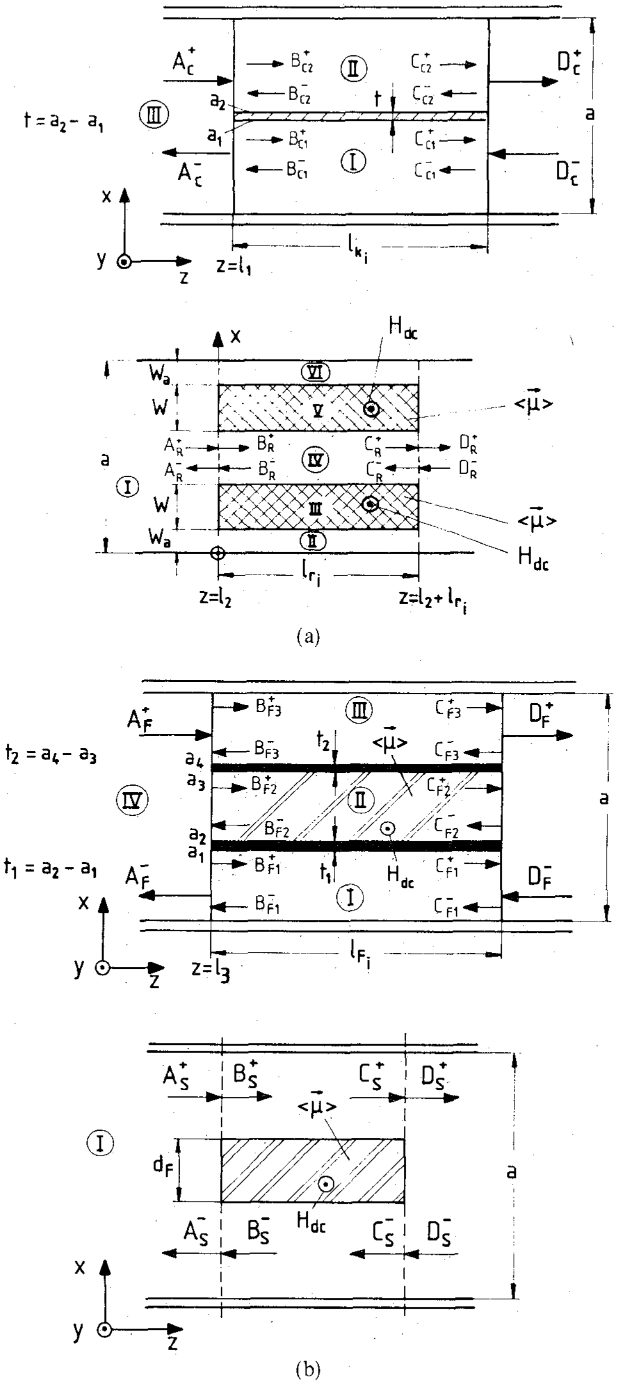

Fig. 2. Key building blocks for the field theory treatment. (a) E-plane metal insert filter with ferrite-loaded resonator sections (lateral air gap w_a considered). (b) Large gap finline filter on a ferrite substrate.

pling effects as well as the finite thickness of all inserts and of the metallization are included.

For computer optimization, the evolution strategy method [15], [21], [28]–[30], i.e., a suitably modified direct-search procedure, is applied where no differentiation step in the optimization process is necessary and hence the problem of local minima may be avoided. Optimized design data and results are presented for magnetically tunable *Ku*-band (12–18 GHz), *Ka*-band (26–40 GHz) and *V*-band (50–75 GHz) metal insert and finline filter examples. The theory is verified by measurements at *Ku*-band waveguide housings (15.799 mm×7.899 mm) for metal insert and finline filters utilizing commercially available TTI-2800 and TTVG-1200 ferrite materials.

II. Theory

For the field theory treatment, the filter structures (Fig. 1) are decomposed into appropriate key building blocks. These are the septate waveguide coupling section [16], [21] with the double-ferrite-slab-loaded resonator region including the air gap region of width w_a, for the metal insert filter type (Fig. 2(a)); and the ferrite-slab-loaded double septate coupling section (metallization of thicknesses t_1, t_2 included) with the single-ferrite-slab-loaded resonator region for the finline filter type (Fig. 2(b)). The overall scattering matrix of the total filter component is calculated by a suitable direct combination [15], [16], [21], [28]–[30] of all single modal scattering matrices of the key building blocks and homogeneous waveguide sections involved. This procedure preserves numerical accuracy, and the number of modes at the discontinuities may be adapted to the specific requirements of each individual step junction, since no symmetry of modes is necessary for this combination method.

For each homogeneous subregion, $\nu = \mathrm{I}$ to IV (Fig. 2), the field equations [23] of the resulting TE_{n0} wave, if a

TE_{m0} wave is incident,

$$\nabla \times \vec{H} = j\omega\epsilon\vec{E} \qquad \nabla\cdot\left(\langle\vec{\mu}\rangle\vec{H}\right) = 0$$

$$\nabla \times \vec{E} = -j\omega\langle\vec{\mu}\rangle\vec{H} \qquad \nabla\cdot\vec{E} = 0 \tag{1}$$

are derived from the electric field component $\vec{e}_y E_y^{(\nu)}$ expressed as a sum of N eigenmodes [11], [28] satisfying the vector Helmholtz equation and the boundary conditions at the discontinuities in the x direction. The permeability tensor for the assumed magnetization in the y direction takes the form [22], [32], [33]

$$\langle\vec{\mu}\rangle = \begin{bmatrix} \mu_1 & 0 & -j\kappa \\ 0 & \mu_r & 0 \\ j\kappa & 0 & \mu_1 \end{bmatrix} \tag{2}$$

with elements μ_1, μ_r, and κ. The filter types under consideration (Fig. 1) operate below ferrimagnetic resonance; hence, the usual calculation of the tensor elements yields reliable results. For a demagnetized ferrite substrate (i.e., $H_{dc} = 0$), the off-diagonal tensor elements vanish, and the diagonal elements may be approximated by expressions given in [32]. For given external dc biasing fields, the internal magnetic field is calculated taking into account the related demagnetization factors [25], [33].

The high power-handling capability of E-plane ferrite-loaded waveguide circuits requires some criteria to be considered for a suitable choice of the corresponding ferrite material [34]–[36] and biasing dc fields. Ferrites with relatively constant thermal characteristics and low losses may help to avoid midband frequency shifts due to the alternation of the magnetic saturation with high temperatures caused by power dissipation in the magnet coils and by the losses of the material. Subsidiary resonance effects [34]–[36] may be circumvented by an appropriate selection of ferrite materials with a suitable spinwave line width [34]–[36] together with a suitable range of the biasing dc field. In contrast to ferrite devices with a constant biasing field (such as high-power differential phase shifters), where operation between subsidiary and main resonance is recommended [34], [35], for tunable filters utilizing the dc field range starting with $H_{dc} = 0$, operation below subsidiary resonance is more suitable. These considerations require an upper limit for the maximum dc biasing magnetic field, e.g. based on calculations given in [34], to be taken into account. For example, the filters with TTI-2800 ferrite material (Transtech Inc.) for midband frequencies at about $f_0 = 14$ GHz, should be magnetized only up to a maximum level of about $H_{dc\,max} \approx 2.2\cdot10^5$ A/m if high signal level transmission is assumed. The related values $H_{dc\,max}$ for the other material TT86-6000 (Transtech Inc.) and midband frequencies f_0 used in this paper are as follows: for $f_0 \approx 29.7$ GHz (*Ka*-band design), $H_{dc\,max} \approx 4.2\cdot10^5$ A/m; for $f_0 \approx 58.2$ GHz (*V*-band design), $H_{dc\,max} \approx 8.3\cdot10^5$ A/m; and for $f_0 \approx 51.7$ GHz (*V*-band design), $H_{dc\,max} \approx 7.4\cdot10^5$ A/m.

The propagation factor γ_n in the waveguide sections is determined via field matching [23], [28] of the transverse field components along the boundaries in the x direction, together with the relations for the single wavenumbers in the cross-sectional subregions. The requirement that the system determinant be zero results in a transcendental equation for γ_n (equation (A17), given in the Appendix) which is solved numerically [28]. The influence of small lateral air gaps of width w_a (cf. Fig. 2(a)), due to fabrication tolerances, on the filter response, which has been observed in evanescent-mode filters as well [6], [7], is adequately taken into account by extending the field matching method to include the subregions VI and II in Fig. 2(a) for the five-layer resonator regions of lengths l_{ri}.

Matching the transversal field components at the corresponding interfaces of Fig. 2 yields the modal scattering matrices of the corresponding discontinuities. As this procedure is already explicitly described in [15], [16], [21], and [28]–[30], for further details of the method the reader is referred to the literature. The modal scattering matrices of the form

$$\begin{bmatrix} (A^-) \\ (D^+) \end{bmatrix} = \begin{bmatrix} (S_{11}) & (S_{12}) \\ (S_{21}) & (S_{22}) \end{bmatrix} \cdot \begin{bmatrix} (A^+) \\ (D^-) \end{bmatrix} \tag{3}$$

of the key building block structures of finite length (Fig. 2) are obtained by suitably arranging the still unknown normalized amplitude coefficients involved including the homogeneous waveguide sections between the inverse discontinuities. The submatrices of the modal scattering matrix of the E-plane metal insert filter coupling section (Fig. 2(a), upper picture) and of the finline filter resonator section (Fig. 2(b), lower picture), of finite length, are already given in [16] and [28], respectively. The corresponding submatrices of the E-plane metal insert filter resonator section (Fig. 2(a), lower picture) and the finline filter coupling section (Fig. 2(b), upper picture) are given in the Appendix.

The computer-aided design of the filters is carried out by an optimization program which applies a suitably modified direct search procedure, namely the evolution strategy method [15], [16], [21], [28]–[31], where no differentiation step is necessary; hence the problem of local minima may be circumvented. An error function $F(\bar{x})$ to be minimized is defined as

$$F(\bar{x}) = \sum_{\upsilon=1}^{V_{stop}} \left[a_{s\,min}/a_{21}(f_\upsilon)\right]^2 + \sum_{\upsilon=1}^{V_{pass}} \left[a_{21}(f_\upsilon)/a_{p\,max}\right]^2 \stackrel{!}{=} \mathrm{Min} \tag{4}$$

where f_υ are the frequency sample points, and V_{stop} and V_{pass} are the numbers of sample points in the stopband and passband, respectively. A total of 20–30 frequency sample points, both in passband and stopband, has turned out to be sufficient. Values $a_{s\,min}$ and $a_{p\,max}$ are the given minimum stopband and maximum passband attenuation, respectively, and $a_{21} = -20\cdot\log(|S_{21}|)$ is the insertion loss calculated at the frequency f_υ.

For given waveguide housing dimensions a, b, given thicknesses of the ferrite slabs, fins, or metal inserts, respectively, and a given number of resonators, the parameters $\bar{x}$ to be optimized are all resonator lengths and lengths of the coupling sections. The initial values for the filter resonator lengths for the optimization structure may be chosen to be $\lambda_g/3$ to $\lambda_g/2$, where λ_g is the guide wavelength of the TE_{10} mode at the given midband frequency; the loading effect of the ferrite slabs is estimated by using the relations for the tensor parameters [22], [32], [33]. For the initial coupling section lengths, the values resulting from the numerical synthesis of the related metal insert filters or finline filters, respectively, without the ferrite-loaded sections [15], [16], [21], have been chosen.

For computer optimization of the filters, the expansion into as many as ten odd eigenmodes (i.e., $TE_{10}, TE_{30}, \cdots, TE_{19\,0}$) within the symmetrical resonator sections has turned out to be sufficient. For each unsymmetrical coupling subregion I, II (Fig. 2(a), upper figure) and I, III (Fig. 2(b), upper figure), however, the related even modes must also be taken into account (i.e., $TE_{10}, TE_{20}, \cdots, TE_{190}$). The final design data are proven through an expansion of 30 odd eigenmodes (and 29 even eigenmodes, respectively). The convergence behavior of the modal method used for ferrite-loaded waveguides has already been demonstrated in [28].

III. Results

Fig. 3(a) shows the calculated and measured filter response of a computer-optimized three-resonator magnetically tunable metal insert filter with two lateral ferrite TTI-2800 slabs (Transtech Inc.) of length $l = 50$ mm and width $w = 1$ mm for two different dc field strengths. The operating midband of the filter may be tuned from about 14.1 GHz to 15.7 GHz. The measured minimum passband insertion loss is about 1 dB. This value compares very well with those reported in literature for the usual types of magnetically tunable filters: evanescent filters (e.g. about 2 dB for a three-section filter at 9 GHz [6]), YIG filters (e.g. about 3–4 dB for a three-section filter at 34 GHz [7]), and hexagonal ferrite filters (e.g. about 6 dB for a two-sphere filter, and about 10 dB for a four-sphere filter, at V-band [39]). In Fig. 3(a), good agreement between theory and measured results may be observed.

Although the technique to use two lateral ferrite slabs along the whole filter section (Fig. 3(a)) may be more convenient concerning a simple manufacturing of the component, improved stopband characteristics of this filter type are obtained by a modified performance (Fig. 3(b)), where only the resonator sections are loaded with the ferrite slabs. The improved tunable E-plane metal insert filter design (Fig. 3b) avoids the undesired secondary effect of the reduction of the cutoff frequency by the ferrite loading for the below-cutoff coupling sections of the filters; hence, direct coupling of modes along the strip section with increasing frequency is circumvented within the waveguide band under consideration. Moreover, the modified filter type (Fig. 3(b)) where the ferrite slabs are

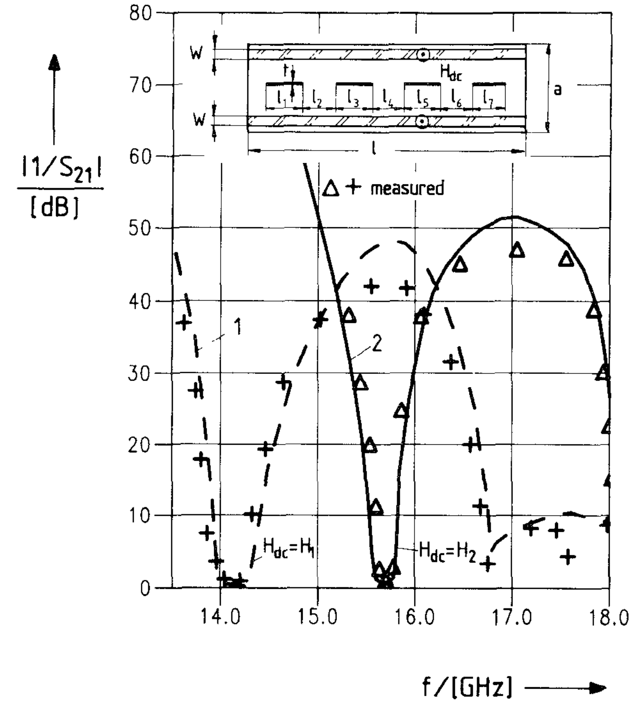

(a)

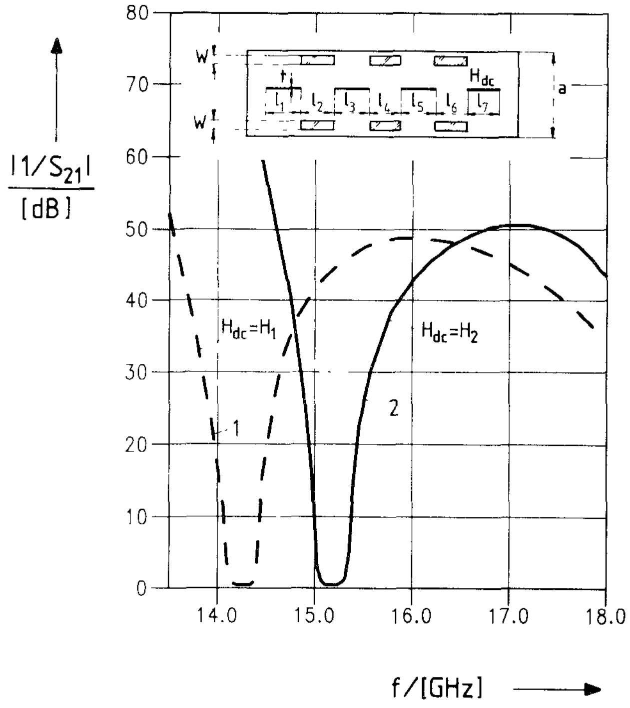

(b)

Fig. 3. Computer-optimized Ku-band magnetically tunable E-plane metal insert filter. Calculated and measured filter response. Design data:

Ferrite TTI-2800, $a = 2b = 15.799$ mm, $t = 0.19$ mm, $l = 50$ mm, $w = 1$ mm, $l_1 = l_7 = 3.59$ mm, $l_2 = l_6 = 8.916$ mm, $l_3 = l_5 = 9.417$ mm, $l_4 = 8.921$ mm, $H_1 = 0$, $H_2 = 1.72 \cdot 10^5$ A/m.

(a) Filter with two lateral ferrite slabs of length l. (b) Filter of improved performance with six lateral ferrite slabs (only in the resonator sections).

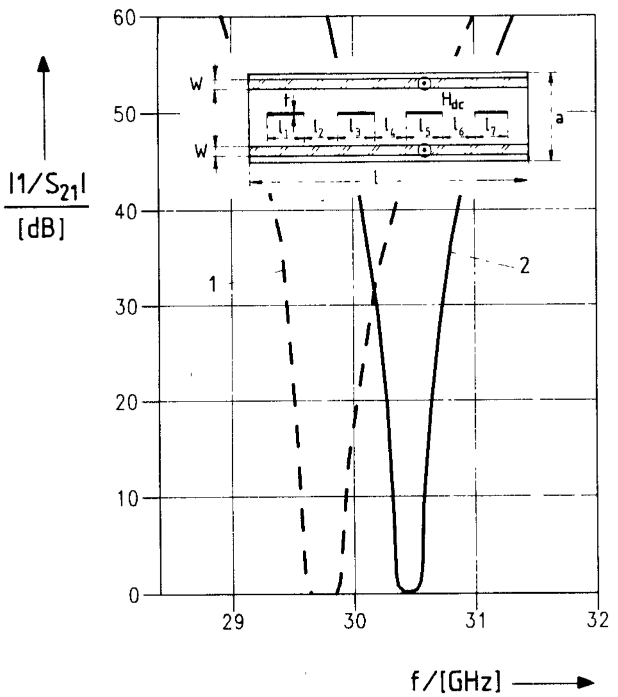

(a)

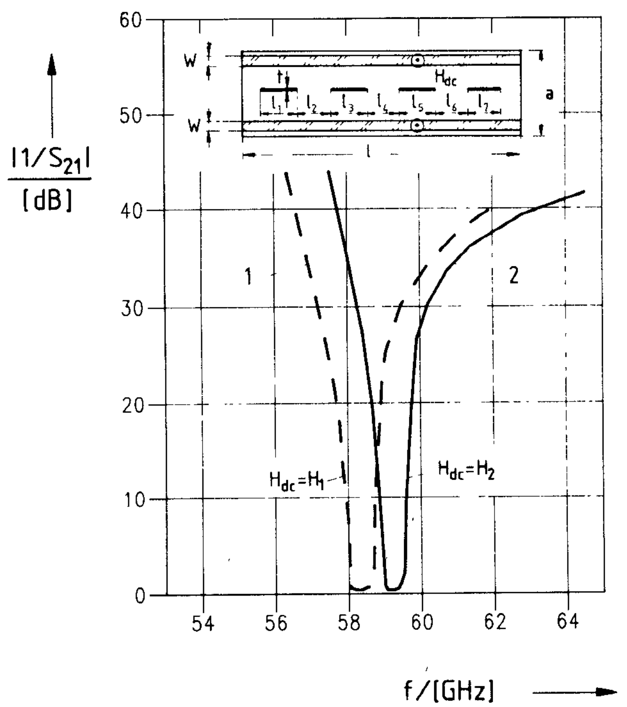

(b)

Fig. 4. Computer-optimized magnetically tunable E-plane metal insert filters. Calculated filter response.

(a) Ka-band design. Design data:

Ferrite TT86-6000, $a = 2b = 7.112$ mm, $t = 0.51$ mm, $l_1 = l_7 = 1.009$ mm, $l_2 = l_6 = 4.778$ mm, $l_3 = l_5 = 3.870$ mm, $l_4 = 4.796$ mm, $H_1 = 0$, $H_2 = 2\cdot 10^5$ A/m, $w = 0.5$ mm.

(b) V-band design. Design data:

Ferrite TT86-6000, $a = 2b = 3.76$ mm, $t = 0.1$ mm, $l_1 = l_7 = 0.708$ mm, $l_2 = l_6 = 2.243$ mm, $l_3 = l_5 = 2.260$ mm, $l_4 = 2.250$ mm, $H_1 = 0$, $H_2 = 8\cdot 10^5$ A/m, $w = 0.25$ mm.

mounted only within the resonator sections achieves still lower insertion losses.

Fig. 4 shows the filter responses of computer-optimized, magnetically tunable, three-resonator E-plane metal insert filters for millimeter-wave applications. The Ka-band design (Fig. 4(a)) with a WR28 waveguide housing (7.112 mm$\times$3.556 mm) uses lateral ferrite TT86-6000 slabs (Transtech Inc.) of widths $w = 0.5$ mm for two different dc field strengths (curves 1, 2). The operating midband of the filter may be tuned within about 29.7 and 30.4 GHz. The V-band design (Fig. 4(b)) with a WR15 housing (3.76 mm$\times$1.88 mm) is based on lateral ferrite slabs of the same material but with a reduced width of $w = 0.25$ mm. Ferrite materials with thicknesses appropriate for millimeter waves may efficiently be fabricated by e.g. arc-plasma-spray processing techniques [37], [38]. The different field strengths considered (curves 1, 2) yield tuning ranges of the operating midband of the filter within about 58.3 and 59.3 GHz (Fig. 4(b)).

The filter responses of computer-optimized millimeter-wave large-gap finline filters on TT86-6000 ferrite substrates are shown in Fig. 5. The Ka-band design (Fig. 5(a)) provides a tuning range from about 29.1 to 30.0 GHz. For the V-band design (Fig. 5(b)), the related values are 51.9 and 53.3 GHz. The millimeter-wave tunable E-plane metal insert filter (Fig. 4(b)) and large-gap finline filter (Fig. 5(b)) designs achieve good constancy in the response shape as the center frequency is varied. Moreover, lower insertion losses may be achieved than with the usual hexagonal ferrite designs [8]–[10], [39].

The theory presented for the large-gap finline filter on a ferrite substrate is verified by measured results of an optimized magnetically tunable three-resonator Ku-band filter on a TTVG-1200 substrate (Fig. 6(a)). The measured minimum insertion losses are about 1.3 dB in the first and 2.3 dB in the second passband. As all relevant parameters, such as higher order mode interactions and the influence of the metallization thicknesses, are included in the design theory, the theoretically predicted values agree well with measured results. The components of the fabricated filter are shown in Fig. 6(b). These comprise the R140 waveguide housing (15.799 mm$\times$7.899 mm) together with the biasing magnet, and the photoetched finline filter structure on the ferrite TTVG-1200 substrate with a chromium/gold reinforced metallization with a total thickness $t = 15$ μm.

IV. Conclusions

A rigorous field theory is applied for the optimum design and improved performance of millimeter-wave ferrite-loaded, magnetically tunable E-plane metal insert filters and large-gap finline filters on a ferrite substrate. Improved stopband characteristics for tunable E-plane metal insert filters are obtained by loading only the resonator sections with ferrite slabs. Large-gap finline filters on a ferrite substrate of reduced width achieve low-insertion-loss designs. Moreover, good constancy of the response shape, as the center frequency is varied, may be stated. Since all relevant parameters, such as higher order

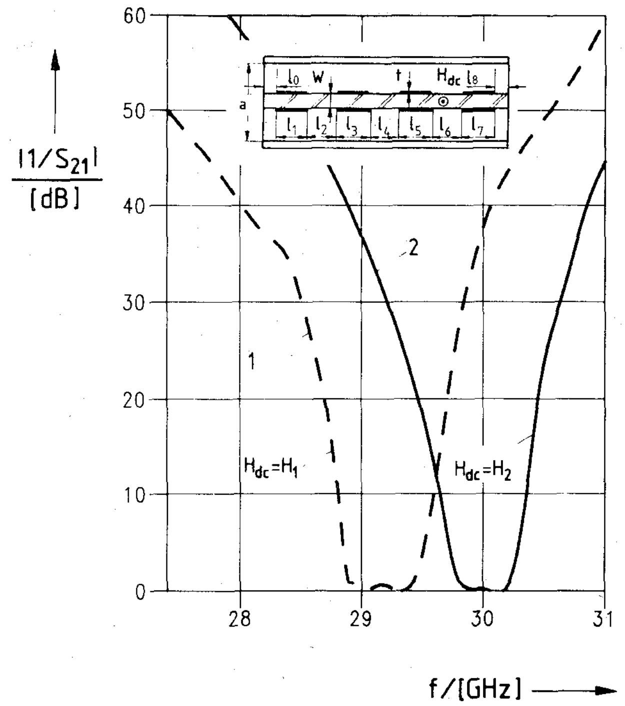

(a)

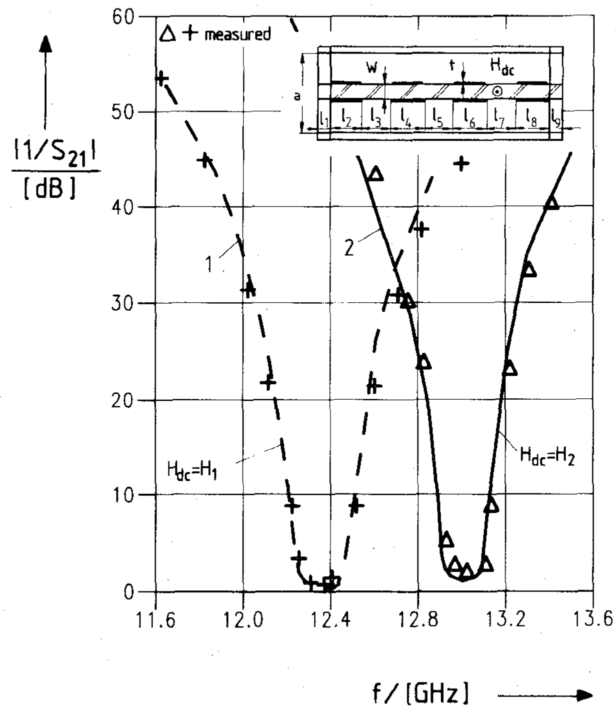

(a)

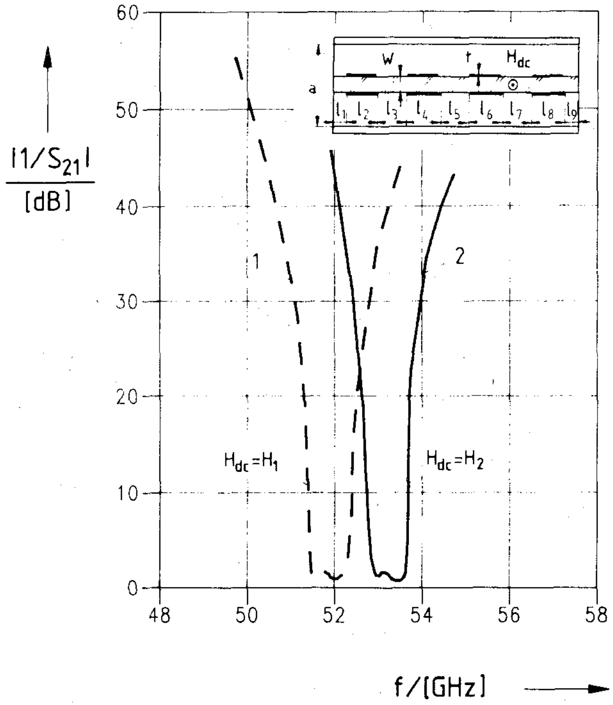

(b)

Fig. 5. Computer-optimized magnetically tunable large-gap finline filter on ferrite substrate. Calculated filter response.

(a) *Ka*-band design. Design data:

Ferrite TT86-6000, $a = 2b = 7.112$ mm, $t = 10$ μm, $l_0 = l_8 = 0.041$ mm, $l_1 = l_7 = 0.870$ mm, $l_2 = l_6 = 2.12$ mm, $l_3 = l_5 = 2.814$ mm, $l_4 = 2.226$ mm, $H_1 = 0$, $H_2 = 2 \cdot 10^5$ A/m, $w = 0.5$ mm.

(b) *V*-band design. Design data:

$l_1 = l_9 = 11.016$ mm, $l_2 = l_8 = 0.33$ mm, $l_3 = l_7 = 1.457$ mm, $l_4 = l_6 = 1.462$ mm, $l_5 = 1.459$ mm, $H_1 = 0$, $H_2 = 6 \cdot 10^5$ A/m, $w = 0.22$ mm.

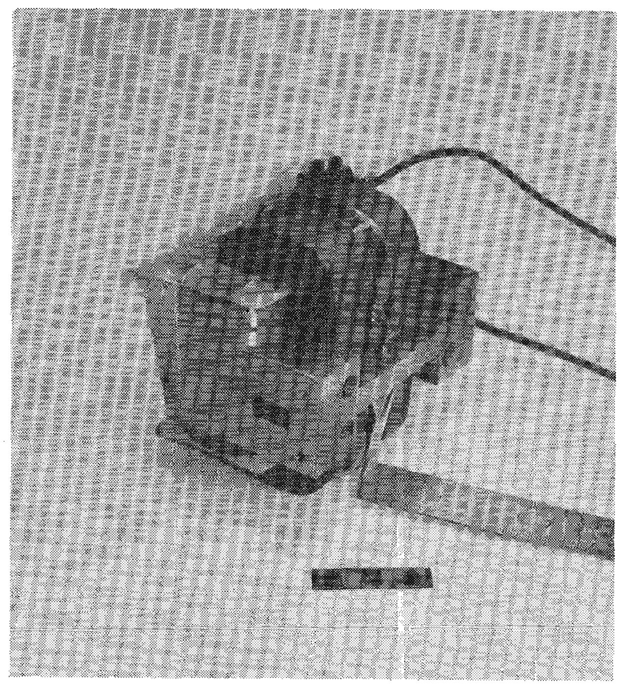

(b)

Fig. 6. Computer-optimized *Ku*-band magnetically tunable large-gap finline filter. Design data:

Ferrite TTVG-1200, $a = 2b = 15.799$ mm, $t = 15$ μm, $l_1 = l_9 = 1.96$ mm, $l_2 = l_8 = 2.136$ mm, $l_3 = l_7 = 6.157$ mm, $l_4 = l_6 = 7.262$ mm, $l_5 = 6.204$ mm, $H_1 = 0$, $H_2 = 2.3 \cdot 10^5$ A/m, $w = 0.7$ mm.

(a) Calculated and measured filter response. (b) Components of a realized magnetically tunable filter: R140 waveguide housing together with the biasing magnet, and the photoetched filter structure on ferrite TTVG-1200 substrate with 15 μm metallization thickness.

mode interactions and the influence of an additional air gap between ferrite slabs and the waveguide walls for the metal insert filter and the metallization thickness for the finline filter, are included in the design theory, the theoretical predicted values agree well with measured results.

Appendix
Scattering Coefficients in (3)

A. E-Plane Metal Insert Filter Resonator Section

$$(S_{11}^R) = (S_{22}^R) = (S_{11}^0) + (S_{12}^0)(R) \cdot \left[(U) - (S_{22}^0)(R)(S_{22}^0)(R)\right]^{-1} \cdot (S_{22}^0)(R)(S_{21}^0) \quad \text{(A1)}$$

$$(S_{12}^R) = (S_{21}^R) = (S_{12}^0)(R) \cdot \left[(U) - (S_{22}^0)(R)(S_{22}^0)(R)\right]^{-1}(S_{21}^0) \quad \text{(A2)}$$

with the following abbreviations:

$$(S_{11}^0) = (D_E)^{-1}(L_E)2(M) - (U) \quad \text{(A3)}$$

$$(S_{12}^0) = (D_E)^{-1}(L_E)\{(U) + (M) \cdot \left[(D_H)^{-1}(L_H) - (D_E)^{-1}(L_E)\right]\} \quad \text{(A4)}$$

$$(S_{21}^0) = 2(M) \quad \text{(A5)}$$

$$(S_{22}^0) = 2(M)(D_H)^{-1}(L_H) - (U) \quad \text{(A6)}$$

$$(M) = \left[(D_E)^{-1}(L_E) + (D_H)^{-1}(L_H)\right]^{-1}. \quad \text{(A7)}$$

The elements of matrices (R), (L_E), and (L_H) are given by

$$(R)_{kk} = \exp(-\gamma_k \cdot l_R) \quad \text{(A8)}$$

$$(L_E)_{mk} = E_k^{(\mathrm{II})} I_{mk}^{(\mathrm{I})} + E_k^{(\mathrm{III})} I_{mk}^{(\mathrm{II})} + F_k^{(\mathrm{III})} I_{mk}^{(\mathrm{III})} + E_k^{(\mathrm{IV})} I_{mk}^{(\mathrm{IV})} \quad \text{(A9)}$$

$$(L_H)_{mk} = E_k^{(\mathrm{II})} \frac{j\gamma_k}{\omega\mu_0\mu_{\mathrm{eff}}} I_{mk}^{(\mathrm{I})} - E_k^{(\mathrm{II})} \frac{\frac{\kappa}{\mu_1} k_{Fk}}{\omega\mu_0\mu_{\mathrm{eff}}} J_{mk}^{(\mathrm{I})} + \frac{j\gamma_k}{\omega\mu_0}\left[E_k^{(\mathrm{III})} I_{mk}^{(\mathrm{II})} + F_k^{(\mathrm{III})} I_{mk}^{(\mathrm{III})}\right] + E_k^{(\mathrm{IV})} \frac{j\gamma_k}{\omega\mu_0\mu_{\mathrm{eff}}} I_{mk}^{(\mathrm{IV})} + E_k^{(\mathrm{IV})} \frac{\frac{\kappa}{\mu_1} k_{Fk}}{\omega\mu_0\mu_{\mathrm{eff}}} J_{mk}^{(\mathrm{IV})} \quad \text{(A10)}$$

with D_E, D_H, E_k, F_k, and $\mu_{\mathrm{eff}} = \mu_2$ given in [28], and with the coupling integrals

$$I_{mk}^{(\mathrm{I})} = \int_0^w \sin(k_{Fk}x) u_m(x)\, dx \quad \text{(A11)}$$

$$I_{mk}^{(\mathrm{II})} = \int_w^{a-w} \sin(k_{Lk}x) u_m(x)\, dx \quad \text{(A12)}$$

$$I_{mk}^{(\mathrm{III})} = \int_w^{a-w} \cos(k_{Lk}x) u_m(x)\, dx \quad \text{(A13)}$$

$$I_{mk}^{(\mathrm{IV})} = \int_{a-w}^{a} \sin(k_{Fk}(a-x)) u_m(x)\, dx \quad \text{(A14)}$$

$$J_{mk}^{(\mathrm{I})} = \int_0^w \cos(k_{Fk}x) u_m(x)\, dx \quad \text{(A15)}$$

$$J_{mk}^{(\mathrm{IV})} = \int_{a-w}^{a} \cos(k_{Fk}(a-x)) u_m(x)\, dx. \quad \text{(A16)}$$

The propagation factor γ_k is calculated by the corresponding transcendental equation of the cross section eigenvalue problem:

$$\begin{aligned}
f(\gamma_n) &= \sin[k_{Ln}(a - 2w - 4w_a)] \sin^2(k_{Fn}w) \cdot \left[\left(\frac{A_{LF}}{2}\right)^2 - \frac{1}{2}\left\{\frac{\mu_{\mathrm{eff}}\left(\frac{\kappa}{\mu_1}\right)\gamma_n}{k_{Ln}}\right\}^2\right] \\
&+ \left[\frac{k_{Fn}\mu_{\mathrm{eff}}\cos(k_{Fn}w)\sin\left(k_{Ln}\left(\frac{a}{2} - w\right)\right)}{k_{Ln}}\right]^2 \\
&- \left[\frac{A_{FL}\sin(k_{Fn}w)}{2}\right]^2 \sin[k_{Ln}(a - 2w)] \\
&- \left[\frac{\sin(k_{Fn}w)}{2}\right]^2 A_{LF}A_{FL}\sin(2k_{Ln}w_a) \\
&+ \frac{\mu_{\mathrm{eff}}k_{Fn}A_{LF}}{4k_{Ln}}\sin(2k_{Fn}w)\sin\left[k_{Ln}\left(\frac{a}{2} - w\right)\right] \cdot \left\{\sin\left[k_{Ln}\left(\frac{a}{2} - w - 2w_a\right)\right] + \cos\left[k_{Ln}\left(\frac{a}{2} - w - 2w_a\right)\right]\right\} \\
&+ \frac{\mu_{\mathrm{eff}}k_{Fn}A_{FL}}{4k_{Ln}}\sin(2k_{Fn}w)\sin\left[k_{Ln}\left(\frac{a}{2} - w\right)\right] \cdot \left\{\cos\left[k_{Ln}\left(\frac{a}{2} - w\right)\right] - \sin\left[k_{Ln}\left(\frac{a}{2} - w\right)\right]\right\}
\end{aligned} \quad \text{(A17)}$$

$$A_{LF} = \mu_{\mathrm{eff}}^2 + \frac{\gamma_n^2}{k_{Ln}^2}\left(\frac{\kappa}{\mu_1}\right)^2 - \left[\frac{k_{Fn}}{k_{Ln}}\right]^2 \quad \text{(A18)}$$

$$A_{FL} = \mu_{\mathrm{eff}}^2 - \frac{\gamma_n^2}{k_{Ln}^2}\left(\frac{\kappa}{\mu_1}\right)^2 + \left[\frac{k_{Fn}}{k_{Ln}}\right]^2. \quad \text{(A19)}$$

$$k_{Ln}^2 = \gamma_n^2 + k_0^2$$

$$k_{Fn}^2 = \gamma_n^2 + k_0\epsilon_f\mu_{\mathrm{eff}} \qquad k_0^2 = \omega^2\mu_0\epsilon_0.$$

B. Finline Coupling Section

$$(S_{11}^F) = (S_{22}^F) = -\{(U) - [(U) - (E)]^{-1}(W) \cdot [(U) - (E)]^{-1}(W)\}^{-1} \cdot \{[(U) - (E)]^{-1}(W)[(U) - (E)]^{-1} \cdot (W) + [(U) - (E)]^{-1}[(U) + (E)]\} \quad \text{(A20)}$$

$$(S_{12}^F) = (S_{21}^F) = -\{(U) - [(U) - (E)]^{-1}(W) \cdot [(U) - (E)]^{-1}(W)\}^{-1} \cdot \{[(U) - (E)]^{-1}(W)[(U) - (E)]^{-1} \cdot [(U) + (E)]^{-1} + [(U) - (E)]^{-1}(W)\} \quad \text{(A21)}$$

with the matrix coefficient

$$(E) = \sum_{n=1}^{3} \left(N_E^{(n)}\right)^2 \left(R^{(n)}\right)\left[\left(R^{(n)}\right)\left(R^{(n)}\right) - (U)\right]^{-1} \cdot \left(N_H^{(n)}\right)^{-1} \tag{A22}$$

$$(W) = \sum_{n=1}^{3} \left(N_E^{(n)}\right)\left\{2\left(R^{(n)}\right)\left[\left(R^{(n)}\right)\left(R^{(n)}\right) - (U)\right]^{-1} - (U)\right\}\left(N_H^{(n)}\right)^{-1} \tag{A23}$$

$$\left(N_E^{(n)}\right) = \left(D_E^{(n)}\right)^{-1}\left(L_E^{(n)}\right) \tag{A24}$$

$$\left(N_H^{(n)}\right) = \left(D_H^{(n)}\right)^{-1}\left(L_H^{(n)}\right). \tag{A25}$$

References

[1] G. L. Matthaei, L. Young, and E. M. T. Jones, *Microwave Filters, Impedance-Matching Networks, and Coupling Structures.* New York: McGraw-Hill, 1964, ch. 17.

[2] S. Toyoda, "Variable bandpass filters using varactor diodes," *IEEE Trans. Microwave Theory Tech.*, vol. MTT-29, pp. 356–362, Apr. 1981.

[3] R. F. Fjerstad, "Some design considerations and realizations of iris-coupled YIG-tuned filters in the 12–40 GHz region," *IEEE Trans. Microwave Theory Tech.*, vol. MTT-18, pp. 205–212, Apr. 1970.

[4] Y. Murakami *et al.* "A 0.5–4.0 GHz tunable bandpass filter using YIG film grown by LPE," *IEEE Trans. Microwave Theory Tech.*, vol. MTT-35, pp. 1192–1197, Dec. 1987.

[5] C. K. Green, "A microstrip nonreciprocal tunable YIG-filter," *IEEE Trans. Microwave Theory Tech.*, vol. MTT-16, pp. 484–485, June 1968.

[6] R. F. Skedd and G. Craven, "Magnetically tunable multisection bandpass filters in ferrite-loaded evanescent waveguide," *Electron. Lett.*, vol. 3, pp. 62–63, Feb. 1967.

[7] R. V. Snyder, "Stepped-ferrite tunable evanescent filters," *IEEE Trans. Microwave Theory Tech.*, vol. MTT-29, pp. 364–371, Apr. 1981.

[8] D. Nicholson, "A high performance hexagonal ferrite tunable bandpass filter for the 40–60 GHz region," in *IEEE MTT-S Int. Symp. Dig.*, 1985, pp. 229–232.

[9] F. Reisch *et al.*, "Magnetically tuned Zn2Z filters for the 18–40 GHz range," *IEEE Trans. Magn.*, vol. MAG-11, pp. 1256–1258, Sept. 1975.

[10] M. Lemke and W. Hoppe, "Barium ferrite—A material for millimeter waves," *Mikrowellen Mag.*, vol. 7, pp. 286–290, 1981.

[11] J. Uher, J. Bornemann, and F. Arndt, "Ferrite tunable metal insert filter," *Electron. Lett.*, vol. 23, pp. 804–806, July 1987.

[12] J. Uher, J. Bornemann, and F. Arndt, "Ferrite tunable millimeter wave printed circuit filters," in *IEEE MTT-S Int. Symp. Dig.* (New York), May 1988, pp. 871–874.

[13] J. Meier, "Integrated fin-line millimeter components," *IEEE Trans. Microwave Theory Tech.*, vol. MTT-32, pp. 209–216, Dec. 1974.

[14] Y. Konishi and K. Uenakada, "The design of a bandpass filter with inductive strip—Planar circuit mounted in waveguide," *IEEE Trans. Microwave Theory Tech.*, vol. MTT-22, pp. 869–873, Oct. 1974.

[15] F. Arndt, J. Bornemann, D. Grauerholz, and R. Vahldieck, "Theory and design of low-insertion loss fin-line filters," *IEEE Trans. Microwave Theory Tech.*, vol. MTT-30, pp. 155–163, Feb. 1982.

[16] R. Vahldieck, J. Bornemann, F. Arndt, and D. Grauerholz, "Optimized waveguide *E*-plane metal insert filters for millimeter-wave applications," *IEEE Trans. Microwave Theory Tech.*, vol. MTT-31, pp. 65–69, Jan. 1983.

[17] K. Solbach, "The status of printed millimeter-wave *E*-plane circuits," *IEEE Trans. Microwave Theory Tech.*, vol. MTT-31, pp. 107–121, Feb. 1983.

[18] Y.-C. Shih and T. Itoh, "*E*-plane filters with finite-thickness septa," *IEEE Trans. Microwave Theory Tech.*, vol. MTT-31, pp. 1009–1012, Dec. 1983.

[19] Y.-C. Shih, "Design of waveguide *E*-plane filters with all metal inserts," *IEEE Trans. Microwave Theory Tech.*, vol. MTT-32, pp. 695–704, July 1984.

[20] P. J. Meier, "Integrated finline: The second decade," *Microwave J.*, vol. 28, pp. 31–54, Nov. 1985; also pp. 30–48, Dec. 1985.

[21] F. Arndt *et al.*, "Modal-*S*-matrix method for the optimum design of inductively direct-coupled cavity filters," *Proc. Inst. Elec. Eng.*, vol. 133, pt. H, pp. 341–350, Oct. 1986.

[22] B. K. J. Lax, K. J. Button, and L. M. Roth, "Ferrite phase shifters in rectangular waveguide," *J. Appl. Phys.*, vol. 25, pp. 1413–1421, 1954.

[23] R. E. Collin, *Field Theory of Guided Waves.* New York: McGraw Hill, ch. 6, pp. 85, 174–179, 198–209.

[24] R. F. Harrington and A. I. Villeneuve, "Receprocity relationships for gyrotropic media," *IRE Trans. Microwave Theory Tech.*, vol. MTT-6, pp. 308–310, July 1958.

[25] F. E. Gardiol and A. S. Vander Vorst, "Computer analysis of *E*-plane resonance isolators," *IEEE Trans. Microwave Theory Tech.*, vol. MTT-19, pp. 315–322, Mar. 1974.

[26] F. E. Gardiol, "Anisotropic slabs in rectangular waveguides," *IEEE Trans. Microwave Theory Tech.*, vol. MTT-18, pp. 461–467, Aug. 1970.

[27] A.-M. Khilla and I. Wolff, "Field theory treatment of *H*-plane waveguide junction with triangular ferrite post," *IEEE Trans. Microwave Theory Tech.*, vol. MTT-26, pp. 279–287, 1978.

[28] J. Uher, F. Arndt, and J. Bornemann, "Field theory design of ferrite-loaded waveguide nonreciprocal phase shifters with multisection ferrite or dielectric slab impedance transformers," *IEEE Trans. Microwave Theory Tech.*, vol. MTT-35, pp. 552–560, June 1987.

[29] F. Arndt, J. Bornemann, and R. Vahldieck, "Design of multisection impedance-matched dielectric-slab filled waveguide phase shifters," *IEEE Trans. Microwave Theory Tech.*, vol. MTT-32, pp. 34–38, Jan. 1984.

[30] F. Arndt, A. Frye, M. Wellnitz, and R. Wirsing, "Double dielectric-slab-filled waveguide phase shifter," *IEEE Trans. Microwave Theory Tech.*, vol. MTT-33, pp. 373–381, May 1985.

[31] H. Schmiedel, "Anwendung der Evolutionsoptimierung bei Mikrowellenschaltungen," *Frequenz*, vol. 35, pp. 306–310, Nov. 1981.

[32] J. J. Green and F. Sandy, "A catalog of low power loss parameters and high power threshold for partially magnetized devices," *IEEE Trans. Microwave Theory Tech.*, vol. MTT-22, pp. 645–651, May 1974.

[33] P. Hlawiczka and A. Mortis, "Gyromagnetic resonance graphical design data," *Proc. Inst. Elec. Eng.*, vol. 11, pp. 665–670, 1963.

[34] J. Helszajn and P. N. Walker, "Operation of high peak power differential phase shift circulator at direct magnetic fields between subsidiary and main resonance," *IEEE Trans. Microwave Theory Tech.*, vol. MTT-26, pp. 653–658, July 1978.

[35] J. Helszajn and M. Powlesland, "Low-loss high-peak-power microstrip circulators," *IEEE Trans. Microwave Theory Tech.*, vol. MTT-29, pp. 572–578, May 1981.

[36] M. Suhl, "The non-linear behaviour of ferrites at high signal level," *Proc. Inst. Radio Eng.*, vol. 44, p. 1270, 1956.

[37] D. H. Harris *et al.*, "Polycrystalline ferrite films for microwave applications deposited by arc-plasma," *J. Appl. Phys.*, vol. 41, pp. 1348–1349, Mar. 1970.

[38] Y. S. Wu, F. J. Rosenbaum, and D. H. Harris, "*X*-band microstrip-inserted puck circulator using arc-plasma-sprayed ferrite," *IEEE Trans. Microwave Theory Tech.*, vol. MTT-23, pp. 504–506, June 1975.

[39] D. Nicholson, "Ferrite tuned millimeter wave bandpass filters with high off resonance isolation," in *IEEE MTT-S Int. Symp. Dig.*, (New York), May 1988, pp. 867–870.

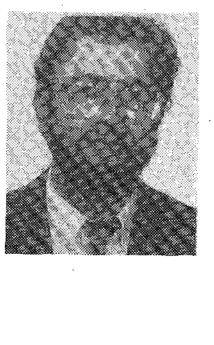

Jaroslaw Uher was born in Klomnice, Poland, on June 2, 1954. He received the M.Sc. degree in electronic engineering from the Technical University of Wroclaw, Poland, in 1978 and the Dr.-Ing. degree in microwave engineering from the University of Bremen, Bremen, West Germany, in 1987.

From 1978 to 1982 his work dealt with planar ferrite engineering at the Institute of Electronic Technology, Technical University of Wroclaw. From 1983 to 1988 he was with the Microwave

Department of the University of Bremen, where his research activities involved field problems of ferrimagnetic slab discontinuities in waveguide structures and the design of ferrite control components and tunable filters. Since September 1988 he has been a research engineer at the University of Ottawa, Ont., Canada. His current activities include millimeter-wave components and systems design.

Fritz Arndt (SM'83) received the Dipl. Ing., Dr. Ing., and Habilitation degrees from the Technical University of Darmstadt, Germany, in 1963, 1968, and 1972, respectively.

From 1963 to 1973, he worked on directional couplers and microstrip techniques at the Technical University of Darmstadt. Since 1972, he has been a Professor and Head of the Microwave Department of the University of Bremen, Germany. His research activities are in the area of the solution of field problems of waveguide, finline, and optical waveguide structures, of antenna design, and of scattering structures.

Dr. Arndt is a member of the VDE and NTG (Germany). He received the NTG award in 1970, the A. F. Bulgin Award (together with three coauthors) from the Institution of Radio and Electronic Engineers in 1983, and the best paper award of the antenna conference JINA 1986 (France).

Jens Bornemann (M'87) was born in Hamburg, West Germany, on May 26, 1952. He received the Dipl.-Ing. and the Dr.-Ing. degrees, both in electrical engineering, from the University of Bremen, West Germany, in 1980 and 1984, respectively.

From 1980 to 1983, he was a Research and Teaching Assistant in the Microwave Department at the University of Bremen, working on quasi-planar waveguide configurations and computer-aided *E*-plane filter design. After a two-year period as a consulting engineer, he joined the University of Bremen again, in 1985, where he was employed at the level of Assistant Professor. Since April 1988, he has been an Associate Professor at the University of Victoria, Victoria, B.C., Canada. His current research activities include microwave system design, active components, and problems of electromagnetic field theory.

Dr. Bornemann was one of the recipients of the A.F. Bulgin Premium of the Institution of Electronic and Radio Engineers in 1983.